Science of the Total Environment 621 (2018) 1533–1541

Contents lists available at ScienceDirect

Science of the Total Environment

journal homepage: www.elsevier.com/locate/scitotenv

Novel approach for removing brominated flame retardant from aquatic environments using Cu/Fe-based metal-organic frameworks: A case of hexabromocyclododecane (HBCD)

Xiang Li [a], Hongli Liu [a], Xiaoshan Jia [b], Guiying Li [a], Taicheng An [a], Yanpeng Gao [a,*]

[a] Guangzhou Key Laboratory of Environmental Catalysis and Pollution Control, School of Environmental Science and Engineering, Institute of Environmental Health and Pollution Control, Guangdong University of Technology, Guangzhou 510006, China
[b] School of Environmental Science and Engineering, Sun Yat-sen University, Guangzhou 510275, China

HIGHLIGHTS

- Two resultant MOFs can successfully remove HBCD from aquatic environment.
- Cu-BTC exhibited a greater affinity to HBCD than Fe-BTC.
- Pseudo second-order kinetic and Langmuir model predicted the experimental data well.
- Hydrophobic interaction contributed to the adsorption.
- The HBCD adsorption enhanced the stability of MOFs in aquatic environment.

GRAPHICAL ABSTRACT

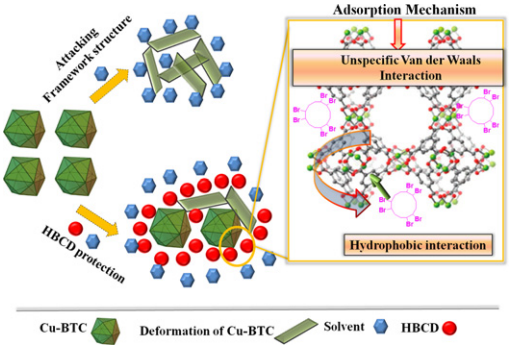

ARTICLE INFO

Article history:
Received 18 July 2017
Received in revised form 7 October 2017
Accepted 9 October 2017
Available online 18 October 2017

Editor: Jay Gan

Keywords:
HBCD
Adsorption mechanism
Water stability
Brominated flame retardant
Metal organic frameworks

ABSTRACT

Cu and Fe based metal-organic frameworks (Cu-BTC and Fe-BTC) were synthesized via a simple solvothermal method and innovatively utilized to remove a typical nonionic brominated flame retardant, hexabromocyclododecane (HBCD), from aquatic environment. Results show that over 80% of HBCD was removed by Cu-BTC within 5 h, which is 1.3 times higher than removal by Fe-BTC. Thermodynamic analysis confirms spontaneous adsorption of HBCD onto the metal-organic frameworks (MOFs). Furthermore, the Gibbs free energy of Cu-BTC (−9.11 kJ/mol) is more negative than that of Fe-BTC (−5.04 kJ/mol). Both adsorption isotherms of HBCD onto Cu-BTC and Fe-BTC followed the Langmuir model, indicating a typical monomolecular-layer adsorption mechanism. In addition, the water stability test of these MOFs shows that the collapse of the Cu-BTC crystal structure is significantly hindered in the aquatic environment due to adsorption of the hydrophobic HBCD. The proposed adsorption mechanism includes van der Waals and hydrophobic interactions. These findings demonstrate that Cu/Fe-BTC are promising adsorbents for the removal of hydrophobic organic pollutants from aquatic environments, and may further improve the understanding of MOF materials for environmental applications.

© 2017 Elsevier B.V. All rights reserved.

1. Introduction

As one of the high production volume of brominated flame retardants (BFRs), 1,2,5,6,9,10-hexabromocyclododecane (HBCD) is

* Corresponding author.
E-mail address: gaoyp2016@gdut.edu.cn (Y. Gao).

https://doi.org/10.1016/j.scitotenv.2017.10.075
0048-9697/© 2017 Elsevier B.V. All rights reserved.

frequently used for fire protection of laminates in printed circuit boards, and plastics in electrical and electronic equipment (Marvin et al., 2011). It is estimated that the production volume of HBCDs was 28,000 tons in 2011, with the main market share in Europe and China (UNEP, 2013). Due to widespread use, HBCD is frequently detected in various environmental matrices. In particular, HBCD is found at very high levels in water near e-waste dismantling sites (Gao et al., 2011) and in areas where this compound is produced or used (Eguchi et al., 2013, Li et al., 2012). Growing evidence indicates that HBCD affects the nervous system, lipid metabolism, oxidative stress and the reproductive processes of aquatic organisms (Cantón et al., 2008, Ema et al., 2008, Saegusa et al., 2009). Additionally, due to its persistent and accumulative properties, in 2013 HBCD was listed in the Stockholm Convention as a persistent organic pollutant (POP) (UNEP, 2013). Therefore, it is highly desirable and imperative to identify a cost-effective technology to remove HBCD from aquatic environments.

Removal of HBCD from contaminated water using adsorption, biotransformation and photocatalytic degradation has been previously studied (Gerecke et al., 2006, Heeb et al., 2013, Peng et al., 2015, Zhang et al., 2014, Zhou et al., 2014). Among these methods, adsorption technology has proven to be a competitive method due to its low cost, simplicity of design and low harmful secondary products (Khan et al., 2013). To date, conventional adsorbents, such as active carbons, organoclays, bio-chars and polymeric resins have been employed to remove organic contaminants from aquatic environments (Cabreralafaurie et al., 2015; Fasfous et al., 2010; Hofer, 2011; Solanki and Boyer, 2017; Zhang et al., 2013). Unfortunately, these alternative strategies seem to still suffer from inherent limitations, such as a small adsorption capacity, lack of selectivity and an inability to be recycled (Xiao et al., 2014).

Porous metal-organic frameworks (MOFs) are promising materials for adsorption-related applications in environmental fields. Particularly, copper- and iron-benzene-1,3,5-tricarboxylate (Cu-BTC and Fe-BTC) are important MOF materials due to their thermal stability up to 240 °C and their large square-shaped pores, which confers huge porosity (Bo Xiao et al., 2007, Chui and Williams, 1999, Dathe et al., 2005, Karra and Walton, 2008, Liang et al., 2009, Petit and Bandosz, 2012). Cu/Fe-BTC have demonstrated good gas storage performance by adsorbing small gas molecules, such as NH_3, H_2S, NO_2, SO_2, CO_2 and CO (Bo Xiao et al., 2007, Dathe et al., 2005, Karra and Walton, 2008, Li et al., 2011, Liang et al., 2009, Petit and Bandosz, 2012). Furthermore, they are promising compounds for adsorptive separation of light hydrocarbons from the gas phase (Autie-Castro et al., 2015; Zukal et al., 2015).

Although there has been extensive research into the application of Cu/Fe-BTC for gas adsorption, few reports have focused on the capabilities of these compounds to remove contaminants from the aqueous phase. These compounds were considered unstable in aqueous systems because Cu/Fe-BTC coordination bonds were thought to be easily attacked by water molecules. Additionally, existing research in aquatic environments shows the adsorption of arsenic (As^{5+}) over Fe-BTC and explains the MOF adsorption mechanism acting as host-guest interactions (Zhu et al., 2012); however, electrostatic interactions are the dominated mechanism during adsorption of methylene blue over Cu-BTC (Lin et al., 2014b). Overall, these results mainly focused on the adsorption of ionic pollutants through electrostatic/charge interactions; however, most emerging contaminants, such as BFRs, are nonionic and the electrostatic/charge interactions between the pollutants and the MOF might be very weak. Accordingly, little is known about the adsorption effect of nonionic organic contaminants on MOFs. Moreover, the existing MOF adsorption mechanisms of various contaminants in aquatic environments are still unclear.

Thus, the objective of this study was to develop an effective adsorption technology for removing nonionic emerging contaminants, such as HBCD, from aquatic environments using synthesized Cu-BTC and Fe-BTC. To that end, a complete profile of the adsorption mechanism was obtained, including detailed adsorption behaviors and kinetics, as well as the adsorption thermodynamic performance of HBCD onto the MOF materials. In addition, the stability of Cu/Fe-BTC in the solute-water system was thoroughly evaluated. X-ray diffraction, scanning electron microscopy, X-ray energy dispersive spectrometer and X-ray photoelectron spectroscopy analysis were employed to characterize the changes in crystal structure of MOFs before and after the adsorption processes. Finally, the adsorption mechanism of HBCD onto MOF materials was proposed.

2. Materials and methods

2.1. Materials

HBCD ($C_{12}H_{18}Br_6$, 97%) was purchased from Sigma-Aldrich Chemical Co., Ltd. (USA). The structural formula of HBCD is given in Fig. S1. HPLC grade methanol was obtained from Thermo-Fisher Co., Ltd. The ultrapure water was obtained directly from a Nanopore UV deionization system (Barnstead/Thermolyne Co., Ltd.; Dubuque, IA, USA). All other chemicals were of analytical grade, unless the stated otherwise.

2.2. Synthesis of Cu/Fe-BTC

Cu-BTC and Fe-BTC were synthesized according to the previously reported procedures (Loera-Serna et al., 2012; Zhu et al., 2012). Briefly, benzenetricarboxylic acid (0.42 g, 2.00 mmol) and $CuNO_3 \cdot 3H_2O$ (0.88 g, 3.65 mmol) or $FeCl_3 \cdot 6H_2O$ (0.66 g, 2.43 mmol) were dissolved in 30 mL DMF/EtOH/H_2O (1:1:1 v/v/v) or 30 mL EtOH/H_2O (1:1 v/v). The resulting mixtures were autoclaved at 105 °C for 24 h and then allowed to cool to room temperature. The blue or dark red powder was collected, washed with 100 mL EtOH/H_2O (1:1 v/v/v), and then dried at 60 °C for 24 h to obtain purified Cu-BTC or Fe-BTC, respectively.

2.3. Characterization of Cu/Fe-BTC

The crystal phase composition of the MOFs before and after adsorption were characterized by X-ray powder diffraction (XRD) using a Rigaku D/MAX2200 diffract meter operated at 30 kV and 30 mA with Cu Kα radiation. The XRD patterns were recorded from 4 to 40 °C of 2θ with a scan speed of 4°/min. MOF surface areas (BET) and pore size distributions were measured by N_2 adsorption-desorption isotherms at 77 K using Micromeritics ASAP 2020 analyzer. Additionally, the surface structure of the MOFs before and after adsorption were measured by scanning electron microscopy (SEM) using a Gemini Leo 1550 instrument attached with an X-ray energy dispersive spectrometer (EDS). Before scanning, all samples were dried and coated with gold to enhance the electron conductivity. Surface chemical properties were also investigated by X-ray photoelectron spectroscopy (XPS) using an ESCALab250 spectrometer with 150 W Al–Kα radiation. The binding energies were referenced to the C1s line at 284.8 eV from adventitious carbon.

The adsorption mixture was analyzed after incubating Cu/Fe-BTC in the HBCD solution for 24 h at room temperature to obtain the adsorption products. The soaked solids were then dried at 45 °C for later characterization.

2.4. Batch adsorption experiments

HBCD stock solutions were prepared by dissolving a known amount of HBCD in methanol. Batch reactions containing the MOF-HBCD mixtures were conducted in 20 mL glass vials sealed with Teflon lined septa. Due to the low solubility of HBCD and the analytical limitations of the instruments, a co-solvent, such as methanol was generally used in the adsorption experiments. The initial concentration of HBCD (methanol:H_2O = 50%:50%) in the final batch reactions was set at approximately 10 mg/L. At selected time intervals, aliquots were withdrawn and then HBCD was extracted using hexane to determine the

final concentration by GC-ECD. Results are quoted as average values of all adsorption experiments, which were performed in triplicate. The HBCD uptake onto MOFs was calculated by Eq. 1:

$$q_t = \frac{(C_0 - C_t)V}{m} \quad (1)$$

where q_t is the adsorbed amount of HBCD (mg/g); C_0 and C_t are the concentrations (mg/L) at the initial and time t (min), respectively; V is the volume (L) of solution; and m is the mass (g) of the MOFs.

2.5. Analytical methods

The concentration of HBCD was quantified using a GC/μECD (SHIMADZU, 2014C) equipped with a DB-5HT column (15 m × 0.25 mm, 0.1 μm film). The injector temperature was set at 260 °C, with a flow rate of 1.0 mL/min. The oven temperature was maintained at 100 °C for 2 min, increased to 280 °C at a rate of 20 °C/min, maintained at 280 °C for 5 min, increased to 310 °C at a rate of 15 °C/min, and then maintained at 310 °C for 10 min. The detector temperature was set at 330 °C.

3. Results and discussion

3.1. Adsorption kinetics of HBCD onto MOFs

Two kinds of MOF adsorbents, Cu-BTC and Fe-BTC, were synthesized under mild conditions and then characterized by SEM, XRD and BET analysis. The XRD patterns showed well-resolved diffraction lines for Cu-BTC, while weak and wide diffraction peaks were observed for Fe-BTC (Fig. S2). Morphologies obtained from SEM exhibited relatively regular block-like particles for Cu-BTC and irregular particles for Fe-BTC (Fig. S3). The BET surface area, pore diameter and volume estimates from N_2 isotherms (Fig. S4) are listed in Table S1. Results demonstrate that the two MOF materials could be synthesized under the mild solvent conditions, as shown in the supplementary materials.

A comparison of the adsorption capacities of the MOFs and activated carbon (Fig.S5) demonstrates that the Cu-BTC removal efficiency of HBCD was 81.5%, which is close to that of the activated carbon (82.36%). These results indicate that Cu-BTC exhibits an excellent ability to remove HBCD from the liquid phase. In addition, MOFs are more selective in adsorptive removal of various toxic components because of their facile functionalization and tunable porosities. The variety of central metal may increase the selectivity for a specific compound from the liquid phase. Thus, the adsorption of HBCD on MOFs was performed in this study. The adsorption kinetics of Cu-BTC and Fe-BTC were tested at an initial HBCD concentration of 10 mg/L in a pH ranging from 4 to 10. The HBCD removal efficiencies of the MOF adsorbents increase as a function of contact time, until a constant value is reached due to the HBCD adsorption onto MOFs (Fig. 1). Adsorption by Cu-BTC took >2.0 h to reach equilibrium, whereas the adsorption equilibrium of Fe-BTC was reached within 0.5 h, indicating a rapid surface adsorption. Thus, it can be concluded that the time to reach the adsorption equilibrium for Cu-BTC is relatively slower than Fe-BTC. However, the opposite trend was observed for the HBCD removal efficiencies of the two MFOs (Fig. 1). Specifically, the highest removal efficiency of Cu-BTC was found to be closed to 80%, which is 1.3 times higher than that of Fe-BTC, thereby indicating that Cu-BTC had a higher adsorption capacity than Fe-BTC. Moreover, this elevated adsorption capacity probably contributes to the higher BET surface area of Cu-BTC (Fig. S4 and Table S1). The regular cubic crystalline material of Cu-BTC results in a highly porous open-framework metal coordination polymer, containing an intersecting three-dimensional system of large square-shaped pores (9 Å) (Chui and Williams, 1999). In this present study, the pore diameter was measured as 8.9 Å for Cu-BTC and 5.3 Å for Fe-BTC (Table S1). Furthermore, the diameter of HBCD was calculated as 7 Å using density functional theories (DFT; supporting information). These data suggest that along with surface adsorption, HBCD molecules may diffuse into the large square-shaped pore system of Cu-BTC. Accordingly, more time is required to reach the adsorption equilibrium as the HBCD molecules diffuse into the pore system. Meanwhile, the large Cu-BTC pores increase the available adsorption active sites and enhance the adsorption capacity of Cu-BTC. Conversely, it is difficult for HBCD molecules to enter into the narrow Fe-BTC pore system due to its irregular particles and agglomerated crystals (Fig. S2). The adsorption of Fe-BTC mainly occurs on the limited surface active sites of the adsorbent, thus the adsorption equilibrium is established quickly. Consequently, Cu-BTC displays a relatively slower adsorption equilibrium time than Fe-BTC.

To further understand the adsorption dynamics of HBCD onto the MOFs, HBCD adsorption kinetics data were fitted with two different kinetic models including pseudo-first-order and pseudo-second-order kinetic models as reported (Chen et al., 2012), as described in Eqs. (2) and (3), respectively.

$$\ln(q_e - q_t) = \ln q_e - k_1 t \quad (2)$$

$$\frac{t}{q_t} = \frac{1}{k_2 q_e^2} + \frac{t}{q_e} \quad (3)$$

where q_e is the adsorption amount (mg/g) at equilibrium; q_t is the adsorption amount (mg/g) at time t (min); and k_1 and k_2 are the pseudo-first-order and pseudo-second-order rate constants, respectively. Fig. S6 illustrates the plots of pseudo-first order kinetics and pseudo-second-order kinetics of HBCD adsorption for both MOFs at different pH values. From the plots, k_1 and k_2 were calculated using the intercepts of pseudo-first order kinetics and pseudo-second-order kinetics, respectively; q_e was calculated with the slope. Results are listed in Table S2. The experimental data fit better to the pseudo-second-order kinetic

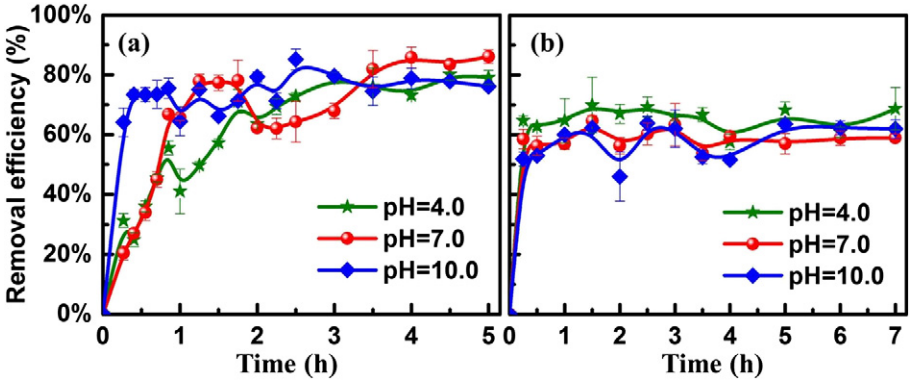

Fig. 1. The adsorption kinetics of HBCD onto (a) Cu-BTC and (b) Fe-BTC.

model, rather than with pseudo-first-order kinetic model (Fig. S6). Moreover, the correlation coefficients (R^2) of the pseudo-second-order kinetic model were obtained as 0.95–0.99, which was higher than those of the pseudo-first-order kinetic model (0.11–0.86). Therefore, the adsorption of HBCD can be better described using a pseudo-second-order kinetic model. In generally, the pseudo-second-order model assumes that the adsorption rate is proportional to the number of active sites on the adsorbent. The initial adsorption rates (k_2) of Cu-BTC were obviously smaller than those of Fe-BTC, yet the calculated adsorption capacities (q_e) of Cu-BTC were larger than those of Fe-BTC (Table S2). Thus, the fitting results are in accordance with the observation from Fig. 1 and are further confirmed by the greater amount of active adsorption sites existing in the large pore system of Cu-BTC.

Due to the complexity of aquatic environments, HBCD exists under various pH conditions. Thus, to evaluate the effect of electrostatic/charge interactions on HBCD adsorption, the adsorption kinetics were performed at three different pH values. The adsorption capacity at pH 4.0, 7.0, and 10.0 of Cu-BTC was 37.5, 39.1 and 31.2 mg/g, respectively; while the adsorption capacity of Fe-BTC was 26.3, 21.5 and 25.2 mg/g, respectively (Table S2). The similar adsorption capacities for each material indicate that HBCD adsorption is independent of pH. This result is contradictory to previous reports indicating that ionic compound adsorption onto MOFs is often highly depended on the pH of the solution because ionization of solutes are effected by the protonation and deprotonation equilibria (Chen et al., 2012; Lin et al., 2014a; Lin et al., 2014b). However, since HBCD is a nonionic hydrophobic organic molecule, the increase of OH^- or H^+ does not change the ionization of HBCD molecule. Thus, the adsorption capacity remains constant in a wide range of pH values. This implies that the electrostatic and base-acid interactions between adsorbents and adsorbed species are not the main adsorption mechanism in this work. Based on the above kinetic results, the two MOFs exhibit a good affinity to HBCD in methanol and water solution under different pH conditions, implying that MOFs have great potential as a water treatment application for waste that contains HBCD.

3.2. Adsorption isotherms and thermodynamics of HBCD adsorption onto MOFs

To further evaluate the HBCD adsorption characteristics, the adsorption isotherms of HBCD onto MOFs were investigated at 298 K. The MOFs (Cu-BTC and Fe-BTC) show excellent affinity to HBCD at equilibrium concentrations ranging from 1.0 to 10.0 mg/L (Fig. 2a). The adsorption capacity increases with increasing equilibrium concentrations. Moreover, Cu-BTC exhibits a higher adsorption capacity for HBCD than Fe-BTC. The elevated adsorption capacity of Cu-BTC is probably due to its higher surface area and larger pore system (Table S1), which allows for access to many more adsorption active sites to remove HBCD from aquatic environment. This finding further confirms the superior adsorption performance of Cu-BTC in removing HBCD within a wide range of equilibrium concentrations.

The Langmuir (Eq. (4)) and Freundlich (Eq. (5)) isotherms models were applied to describe the adsorption equilibrium, according to two previously described empirical equations (Jung et al., 2013):

$$q_e = \frac{q_m K_L C_e}{1 + K_L C_e} \tag{4}$$

$$q_e = K_f C_e^n \tag{5}$$

where C_e is the equilibrium concentration (mg/L); q_e is the amount (mg/g) of HBCD adsorbed onto of adsorbent, per unit mass, at equilibrium; q_m is the maximum adsorption capacity (mg/g) as correlated with monolayer coverage; K_L and K_f are the model constant (L/mg); and n is an indicator of adsorption intensity.

For Langmuir model, linear plots of C_e/q_e versus C_e are shown in Fig. 2b. K_L and q_m were calculated from the slope and intercept of different straight lines, respectively. Results are listed in Table S3. The data fit well with the adsorption of HBCD onto Cu-BTC and Fe-BTC under the experimental conditions ($R^2 \geq 0.98$). Generally, the Langmuir model assumes monolayer adsorption onto a surface, which consists of a finite number of active sites with a uniform energy. Thus, the above data indicates that the adsorptions of HBCD onto Cu/Fe-based MOFs are a typical monomolecular-layer adsorption, with maximum monolayer capacities (q_m) for Cu-BTC and Fe-BTC calculated as 46.5 and 26.8 mg/g, respectively. The specific surface area for the normalized HBCD adsorption capacity was calculated as 0.001 and 0.017 molecule/um^2 for Cu-BTC and Fe-BTC, respectively. The higher adsorption capacity for Fe-BTC suggests that other factors along with surface area also contribute to its excellent performance in the batch experiments. Hydrophobic interaction between benzene rings in Cu/Fe-BTC and hydrophobic compounds are often observed during adsorption. Hence, it is extremely possible that these interactions also contribute MOF adsorption of HBCD, which is a highly hydrophobic compound.

For the Freundlich model, linear plots of Log (C_e) versus Log (q_e) are shown in Fig. 2c. K_f and n were calculated from the slope and intercept, respectively, and listed in Table S3. As shown, the data does not fit well with the adsorption curve over Cu-BTC. Meanwhile, the correlation coefficient ($R^2 \leq 0.7$) of Cu-BTC shows poor agreement with the experimental data, indicating that the Freundlich model fails to explain the Cu-BTC adsorption process. In contrast, the correlation coefficient ($R^2 \geq 0.9$) of Fe-BTC indicates that the Freundlich model can successfully describe this experimental data. Generally, the Freundlich model is used to describe heterogeneous reactions and reversible adsorption rather than monolayer adsorption. Thus, the HBCD reversible adsorption over Fe-BTC is ascribed to a bad crystallization structure, limited adsorption active sites and a heterogeneous surface.

To further shed light on the adsorption by Cu-BTC and Fe-BTC, the adsorption thermodynamic parameters (ΔG_0) were calculated based on the Eq. (6) (Zhu et al., 2012):

$$K_0 = \frac{\alpha_q}{\alpha_c} = \frac{\gamma_s q_e}{\gamma_e C_e} = \frac{q_e}{C_e} \tag{6}$$

where α_q is the activity of HBCD adsorbed onto MOFs; α_c is the activity of HBCD in solution at equilibrium; and γ is the activity coefficient. K_0 is confirmed by plotting $\ln K_0$ vs q_e, and extrapolating q_e to zero. The

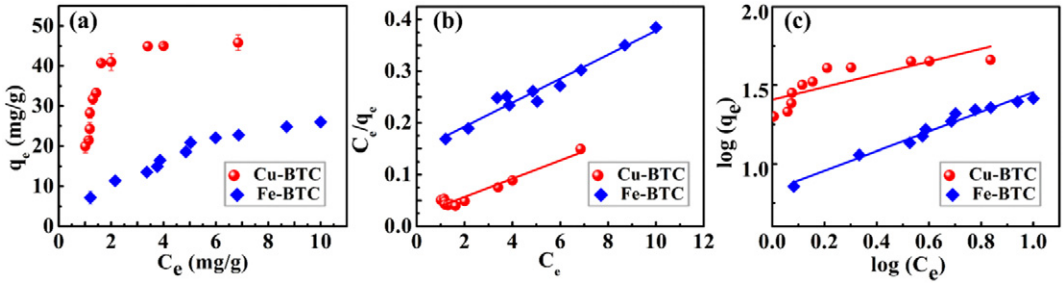

Fig. 2. (a) Adsorption isotherms for HBCD onto Cu-BTC and Fe-BTC; (b) Langmuir plots of the isotherms; (c) Freundlich plots of the isotherms.

straight line is fitted using linear least-squares analysis, with the intercept of vertical axis regarded as $\ln K_0$. The plots of $\ln K_0$ vs q_e are shown in Fig. S7, and the Gibbs energy (ΔG^0) of adsorption was calculated from Eq. (7):

$$\Delta G^0 = -RT\ln K_0 \quad (7)$$

Where R is the ideal gas constant and T is the absolute temperature. The ΔG^0 values of HBCD adsorption onto Cu-BTC and Fe-BTC were calculated as −9.11 and −5.04 kJ/mol, respectively, thereby indicating that HBCD adsorption is a spontaneous process by both Cu-BTC and Fe-BTC. In addition, since the ΔG^0 value of Cu-BTC is more negative than that of Fe-BTC, HBCD interaction with Cu-BTC is stronger than with Fe-BTC, from the theoretical standpoint. Generally, ΔG^0 values range from 0 to −20 and −80 to −400 kJ/mol for typical physical and chemical adsorption, respectively. Thus, both Cu-BTC and Fe-BTC work by physical adsorption rather than chemical adsorption. In summary, the results of the isotherm and thermodynamic studies demonstrate that the pre-synthesized MOF adsorbents for HBCD removal from aquatic environments are effective and reasonable.

3.3. The effect of water molecules on HBCD adsorption

Because the MOFs used in this study were hydrated materials, water molecules in the solvents may have influenced adsorption. Thus, the adsorption mechanism of HBCD on Cu-BTC was investigated using different water-solvents ratios. Due the low solubility of HBCD in water, the ratio of water to methanol (v:v) was set as 50%:50%, 35%:65%, 15%:85% and 0%:100%. The HBCD removal efficiency remained almost unchanged with decreasing water in the solution (Fig. S8); therefore, results indicate that the presence of water molecules did not affect the performance of the MOFs for removing HBCD from the liquid phase. As previously reported, the preferential adsorption site for water on Cu-BTC framework is different from organic molecules; water adsorption mainly occurs near the Cu atoms, while organic molecules preferentially adsorb to organic ligands on the framework (Schlichte et al., 2004). Therefore, competitive adsorption was not observed, thereby confirming that adsorption of HBCD is not influenced by the water-methanol ratio in solvents.

3.4. Proposed adsorption mechanism of HBCD onto MOFs

As demonstrated, HBCD adsorption onto Cu-BTC and Fe-BTC is physical. Furthermore, electrical and acid-base interactions do not influence HBCD adsorption. The theoretical calculation for the HBCD molecular size and the pore size analysis obtained from the N_2 sorption-desorption isotherm implies that the pore system can uptake HBCD from the aquatic environment. However, the higher normalized surface area adsorption capacity for Fe-BTC indicates that other adsorption mechanisms also contribute to HBCD adsorption. Moreover, higher water content in the solvent did not significantly change the adsorption capacity of Cu-BTC. This indicates that the adsorption active site for water molecules is different from that of HBCD molecules, as water adsorption mainly occurs near the Cu atoms of the framework. Thus, the HBCD adsorbs to the benzene rings of the MOF ligands.

To further investigate the microscopic adsorption mechanism, XPS analysis was chosen to study Cu-BTC samples in pure solvent solution and HBCD solution. Cu-BTC is mainly composed of Cu, O and C elements (Fig. S9). After HBCD adsorption, excess Br was observed in the XPS spectra, suggesting that HBCD was successfully adsorbed onto Cu-BTC. Fig. 3 presents high resolution Cu2p, O1s, C1s and Br3d XPS spectra data of Cu-BTC in HBCD solution. The carbon C1s peaks at 284.3 and 288.2 eV correspond to phenyl and carboxyl signals; the oxygen O1s peak at 531.3 eV is assigned to Cu-O-C species; the Cu2p spectra were

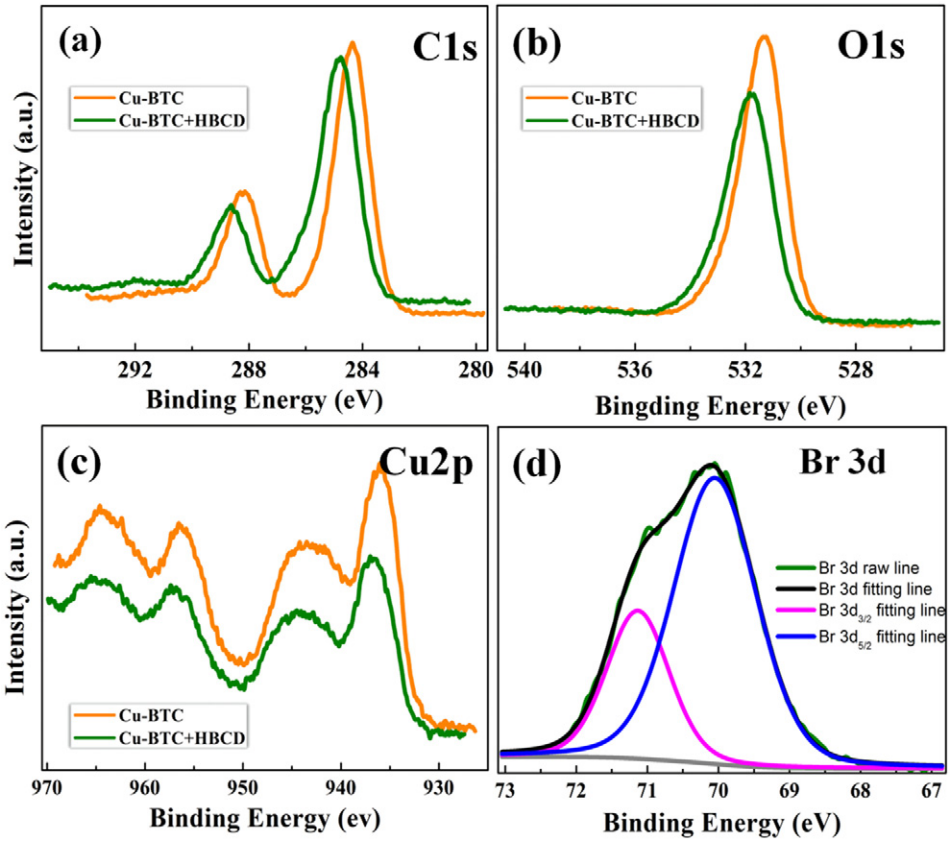

Fig. 3. The XPS spectrum of Cu-BTC and HBCD-Cu-BTC complexes: (a) high resolution of C spectrum; (b) high resolution of O spectrum; (c) high resolution of Cu spectrum; (d) high resolution of Br spectrum.

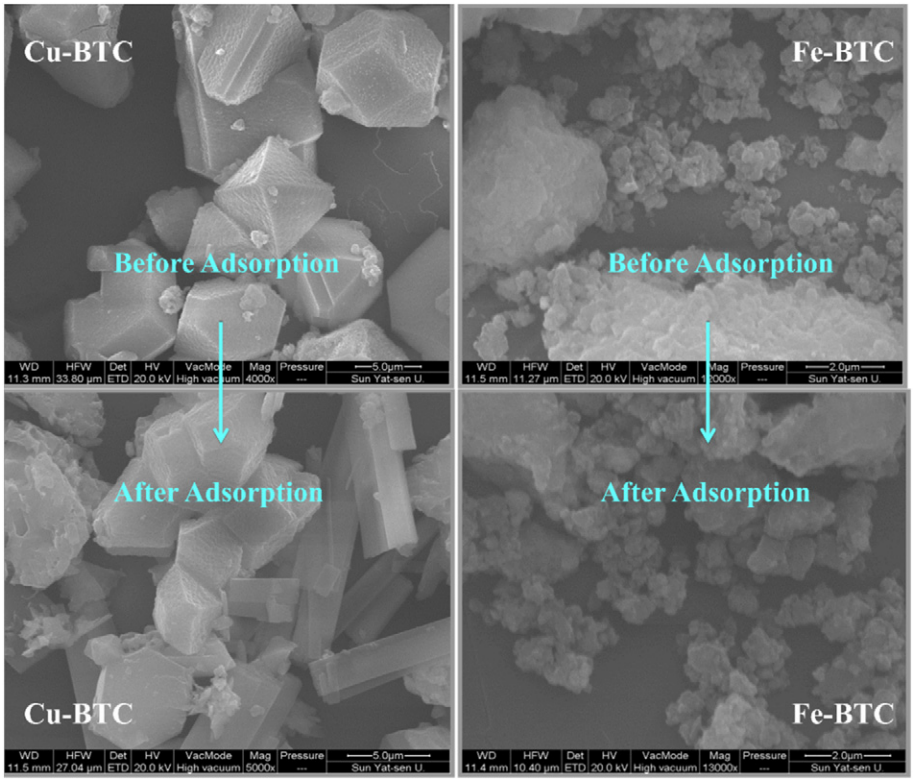

Fig. 4. SEM images for Cu/Fe-based MOFs before and after HBCD adsorption (a) Cu-BTC; (b) Cu-BTC after adsorption; (c) Fe-BTC; (d) Fe-BTC after adsorption.

composed of four peaks centered at 935.3, 943.1, 956.9 and 964.5 eV, which correspond to the $Cu2p_{1/2}$ peak, the satellite $Cu2p_{1/2}$ peak, the $Cu2p_{3/2}$ peak and satellite $Cu2p_{3}/2$ peak, respectively; The B3d spectra were composed of two peaks centered at 70.03 and 71.14 eV, corresponding to the $Br3d_{5/2}$ and $Br3d_{3/2}$ peaks, respectively. When the Cu-BTC in HBCD solution was compared to that of Cu-BTC in pure solvent, no binding energy shift was observed for the Cu2p and CuLMM peaks, whereas the binding energy of the O1s and C1s peaks shifted to the left side (Figs. 3 and S10). This implies that HBCD interaction on the surface of Cu-BTC probably occurs with the organic ligands of Cu-BTC, rather than the open metal sites (Cu^{2+}). Furthermore, quantitative atomic ratios were computed according to the intensities of the O1s and C1s peaks. The quantitative C/Cu surface atomic ratio of Cu-BTC increased from 5.62 to 7.86, which is likely due to the addition of HBCD on the Cu-BTC surface. Additionally, the quantitative O/Cu surface atomic ratio of used Cu-BTC slightly decreased from 4.61 to 3.61, which indicates that the amount of surface oxygen atoms decreased after HBCD adsorption. Previous studies have proven that solvent molecules, such as H_2O, can be adsorbed on the Cu-BTC surface in liquid solution (Gutiérrez-Sevillano et al., 2013). One possible explanation for the decrease in the O/Cu value is that the presence of HBCD inhibits adsorption of the solvent molecules on the Cu-BTC surface, which leads to a decrease in oxygen atoms.

Because HBCD is a non-polar molecule with low water solubility, electrical or acid/base interactions could not be the main adsorption mechanism, as evidenced by the pH-independent HBCD adsorption. Based on the O1s and C1s XPS analysis, hydrophobic interactions between HBCD and the organic MOF ligands (BTC) likely play an important role. It is extremely possible that HBCD adsorption onto the MOF surface increases the organic C atomic ratio while simultaneously creating a more hydrophobic environment, which decreases the affinity of MOF for solvent molecules, such as H_2O.

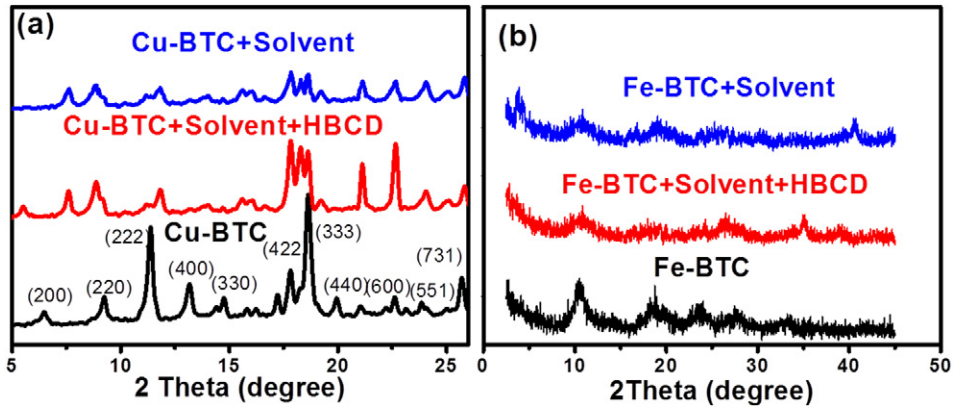

Fig. 5. X-ray diffraction patterns of MOFs before and after HBCD adsorption: (a) Cu-BTC; (b) Fe-BTC.

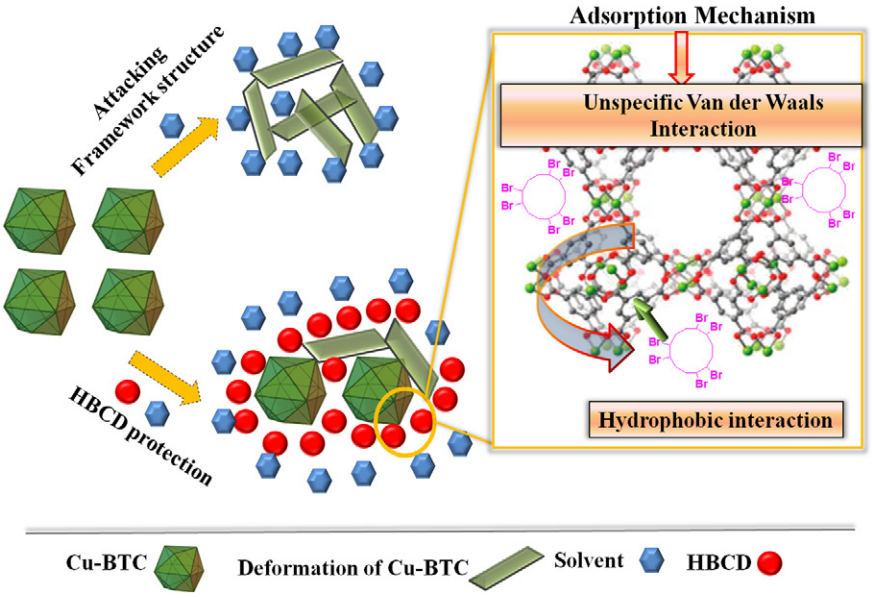

Scheme 1. The proposed adsorption mechanism of HBCD onto Cu-BTC.

3.5. The stability of MOFs during the adsorption processes

The stability of MOFs in aquatic environments is a key factor for their practical application in wastewater treatment. To further understand their stability in the HBCD solution, EDS, SEM and XRD techniques were used to characterize the MOFs before and after adsorption. The elemental composition of MOFs was characterized by EDS analysis (Fig. S11). Prior to adsorption, Br was not observed in the MOFs, whereas the percentage of Br in Cu-BTC and Fe-BTC after HBCD adsorption was measured at 2.49% and 1.18%, respectively. This further confirms that HBCD is successfully adsorbed onto both MOF materials.

In addition, the morphologies and crystal structures of MOFs were characterized by SEM (Fig. 4) and XRD analysis (Fig. 5). For Cu-BTC, some layer-like structures were observed in the SEM images (Fig. 4a and c) after Cu-BTC liquid-phase adsorption. Meanwhile, an obvious decrease in peaks was observed in the XRD patterns (Fig. 5a) of Cu-BTC adsorbed with HBCD. This is due to the instability of Cu-BTC in aqueous solution. For Fe-BTC, no difference in SEM morphology was observed before and after adsorption (Fig. 4b and d), which was likely attributed to the low degree of crystallization of pristine Fe-BTC. However, similar to Cu-BTC, the XRD patterns of Fe-BTC displayed a significant decrease in peaks after HBCD adsorption (Fig. 5b). The above results prove that the initial framework structures of both Cu-BTC and Fe-BTC were significantly altered in the HBCD solution. Previous studies demonstrate that solvent molecules, such as H_2O, can attack the metal atoms of the MOFs, thereby collapsing the framework structure (Li et al., 2016). Thus, during the HBCD liquid-phase adsorption process, there indeed exists some alteration of MOF structures.

To further investigate the structural changes to MOFs in HBCD solution, a comparative XRD study was performed between Cu-BTC in HBCD solution and in pure solution (Fig. 5a). Interestingly, the intensities of the peaks for Cu-BTC in HBCD solution were higher than those of Cu-BTC in pure solvent, which probably due to the existence of HBCD. To further count for the effect of HBCD, the crystallization ratio between Cu-BTC in pure solution and Cu-BTC in HBCD solution was determined by considering the ratio of the sum of the intensity of 10 major peaks: crystallization ratio $I = \sum I_{\text{Cu-BTC used}} / \sum I_{\text{Cu-BTC pristine}}$. The resulting ratios for Cu-BTC in pure solvent solution and Cu-BTC in HBCD solution were 0.57 and 0.89, respectively; thereby suggesting that the collapse of crystal structure was significantly hindered in HBCD solution due to the existence of HBCD. A possible explanation for this phenomenon is that adsorption on the surface of Cu-BTC by HBCD, a nonionic hydrophobic molecule, creates a more hydrophobic environment, which blocks the adsorption of solvent molecules and prevents them from attacking the copper atoms. The increased hydrophobicity resulting from adsorption of organic molecules on MOFs has also been reported for adsorption of oil droplets onto Cu-BTC, where Cu-BTC quickly separates from the water system after adsorption of oil droplets, indicating enhanced surface hydrophobicity of oil droplets associated with Cu-BTC (Lin et al., 2014a). In this study, the XRD and SEM results further confirm that the adsorption of nonionic hydrophobic organic molecules can inhibit solvent molecules from attacking coordinate bonds, thus enhancing the stability of the crystal structure in the aquatic environment (Scheme 1). These findings may facilitate the practical application of organic compound adsorption onto MOFs and provides solid evidence of the instability of MOFs in aquatic environments.

Based on the above results, the main adsorption interaction is attributed to the hydrophobic interaction of HBCD with organic ligands on the MOFs. Furthermore, the open metal site (Cu^{2+} and Fe^{2+}) does not primarily contribute to the adsorption mechanism. Cu-BTC has a greater adsorption performance than Fe-BTC because the large Cu-BTC pore system facilitates increased adsorption. During the initial adsorption stage, Cu-BTC in the HBCD solution system is partly altered and destroyed by H_2O attack. However, with the increase of HBCD adsorption onto the Cu-BTC surface, the adsorbed HBCD may create a more hydrophobic environment on the MOF surface and inhibit the solvent molecules from attacking the MOFs structure, which preserves the

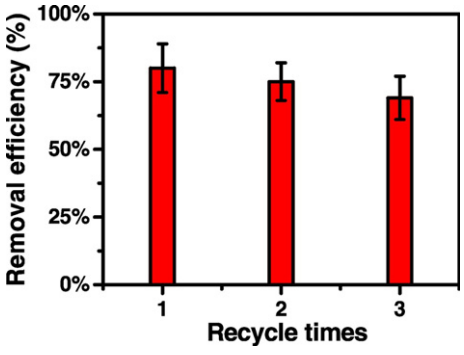

Fig. 6. Effect of recycle times of Cu-BTC on the HBCD removal efficiency (%).

crystal structure to some extent. Additionally, the tentative adsorption mechanism is proposed as van der Waals interactions accompanied by hydrophobic interactions, as summarized in the Scheme 1.

3.6. Cu-BTC regeneration

Previous studies have shown that Cu-BTC hold great potential for water treatment because it can be regenerated with an ethanol solution (Jung et al., 2013). In this study, the used adsorbent was regenerated by washing with an ethanol solution (supporting information). The effect of regeneration times are shown in Fig. 6. In comparison to fresh Cu-BTC, the removal efficiency only decreased by 5% after the first regeneration, while it decreased by 11% following the second regeneration, thus maintaining 65% efficiency. This indicates that Cu-BTC is a recyclable adsorbent for removing HBCD from water because it can be regenerated at least three times following the adsorption process.

3.7. The competition of HA on HBCD adsorption

The effect of natural organic matter (NOM), such as humic acids (HAs), on the adsorption of HBCD onto MOFs was also investigated. HBCD uptake decreased from 40.12 to 25.33 mg/g when the HA concentration increased from 0 to 30 mg/L (Fig. S12). Results indicate that NOM significantly inhibits the adsorption of HBCD onto MOFs. This may be attributed to the competition of HA with HBCD for adsorption sites, thereby reducing HBCD adsorption on MOFs. In order to confirm this, the adsorption of HAs on MOFs was investigated by TOC analysis. Results show that almost 30% of the HAs were successfully removed from water by MOFs, which indicates that MOFs can interact with HAs; therefore, it is extremely possible that the presence of HAs inhibit adsorption of HBCD on MOFs through competitive exclusion.

4. Conclusions

This work demonstrates the feasibility of using MOFs, such as Cu-BTC and Fe-BTC, to remove HBDC from aquatic environments. Cu-BTC exhibits a slower adsorption rate but a higher adsorption capacity, relative to Fe-BTC, because of its crystalline structure. This suggests the greater potential of Cu-BTC for the adsorptive removal of HBCD. The adsorption process follows the pseudo-second order model and is spontaneous, as evidenced by the negative ΔG values for Cu-BTC (-9.11 kJ/mol) and Fe-BTC (-5.04 kJ/mol). Moreover, adsorption of HBCD onto Cu-BTC and Fe-BTC occurs as a typical monomolecular layer, which is better described by the Langmuir model than the Freundlich model. Van der Waals interactions accompanied by hydrophobic interactions are proposed as the adsorption mechanism based on XPS analysis. The crystal structure of the MOFs is preserved in HBCD solution because adsorption of the HBCD molecule creates a hydrophobic environment. Increased hydrophobicity results in H_2O desorption from the MOF surface, thereby preventing H_2O molecules from attacking the framework structure. Thus, it can be concluded that Cu/Fe-BTC are promising adsorbents for the removal of hydrophobic organics from aquatic environments.

Acknowledgements

This work was financially supported by National Natural Science Funds for Distinguished Young Scholars (41425015) and NSFC (41573086, 41603115). There is no conflict of interests.

Appendix A. Supplementary data

Supplementary data to this article can be found online at https://doi.org/10.1016/j.scitotenv.2017.10.075.

References

Autie-Castro, G., Autie, M.A., Rodríguez-Castellón, E., Aguirre, C., Reguera, E., 2015. Cu-BTC and Fe-BTC metal-organic frameworks: role of the materials structural features on their performance for volatile hydrocarbons separation. Colloids Surf. A 481, 351–357.
Cabreralafaurie, W.A., Román, F.R., Hernándezmaldonado, A.J., 2015. Single and multi-component adsorption of salicylic acid, clofibric acid, carbamazepine and caffeine from water onto transition metal modified and partially calcined inorganic-organic pillared clay fixed beds. J. Hazard. Mater. 282 (1), 174–182.
Cantón, R.F., Peijnenburg, A.A., Hoogenboom, R.L., Piersma, A.H., Lt, V.D.V., Van, d.B.M., Heneweer, M., 2008. Subacute effects of hexabromocyclododecane (HBCD) on hepatic gene expression profiles in rats. Toxicol. Appl. Pharmacol. 231 (2), 267–272.
Chen, C., Zhang, M., Guan, Q., Li, W., 2012. Kinetic and thermodynamic studies on the adsorption of xylenol orange onto MIL-101(Cr). Chem. Eng. J. 183 (8), 60–67.
Chui, S.Y., Williams, I.D., 1999. A chemically functionalizable nanoporous material. Science 283 (5405), 1148–1150.
Dathe, H., Peringer, E., Roberts, V., Jentys, A., Lercher, J.A., 2005. Metal organic frameworks based on Cu^{2+} and benzene-1,3,5-tricarboxylate as host for SO_2 trapping agents. C. R. Chim. 8 (3–4), 753–763.
Eguchi, A., Isobe, T., Ramu, K., Tue, N.M., Sudaryanto, A., Devanathan, G., Viet, P.H., Tana, R.S., Takahashi, S., Subramanian, A., 2013. Soil contamination by brominated flame retardants in open waste dumping sites in Asian developing countries. Chemosphere 90 (9), 2365–2371.
Ema, M., Fujii, S., Hiratakoizumi, M., Matsumoto, M., 2008. Two-generation reproductive toxicity study of the flame retardant hexabromocyclododecane in rats. Reprod. Toxicol. 25 (3), 335–351.
Fasfous, I.I., Radwan, E.S., Dawoud, J.N., 2010. Kinetics, equilibrium and thermodynamics of the sorption of tetrabromobisphenol A on multiwalled carbon nanotubes. Appl. Surf. Sci. 256 (23), 7246–7252.
Gao, S.T., Wang, J.Z., Yu, Z.Q., Guo, Q.R., Sheng, G.Y., Fu, J.M., 2011. Hexabromocyclododecanes in surface soils from E-waste recycling areas and industrial areas in South China: concentrations, diastereoisomer- and enantiomer-specific profiles, and inventory. Environ. Sci. Technol. 45 (6), 2093–2099.
Gerecke, A.C., Giger, W., Hartmann, P.C., Heeb, N.V., Kohler, H.P., Schmid, P., Zennegg, M., Kohler, M., 2006. Anaerobic degradation of brominated flame retardants in sewage sludge. Chemosphere 64 (2), 311–317.
Gutiérrez-Sevillano, J.J., Vicent-Luna, J.M., Dubbeldam, D., Calero, S., 2013. Molecular mechanisms for adsorption in Cu-BTC metal organic framework. J. Phys. Chem. C 117 (21), 11357–11366.
Heeb, N.V., Zindel, D., Graf, H., Azara, V., Schweizer, W.B., Geueke, B., Kohler, H.P.E., Lienemann, P., 2013. Stereochemistry of LinB-catalyzed biotransformation of delta-HBCD to 1R,2R,5S,6R,9R,10S-pentabromocyclododecanol. Chemosphere 90 (6), 1911–1919.
Hofer, W., 2011. A review of biochars' potential role in the remediation, revegetation and restoration of contaminated soils. Environ. Pollut. 159 (12), 3269–3282.
Jung, B.K., Hasan, Z., Jhung, S.H., 2013. Adsorptive removal of 2,4-dichlorophenoxyacetic acid (2,4-D) from water with a metal–organic framework. Chem. Eng. J. 234, 99–105.
Karra, J.R., Walton, K.S., 2008. Effect of open metal sites on adsorption of polar and nonpolar molecules in metal-organic framework Cu-BTC. Langmuir 24 (16), 8620–8626.
Khan, N.A., Hasan, Z., Jhung, S.H., 2013. Adsorptive removal of hazardous materials using metal-organic frameworks (MOFs): a review. J. Hazard. Mater. 244, 444–456.
Li, J.R., Ma, Y., Mccarthy, M.C., Sculley, J., Yu, J., Jeong, H.K., Balbuena, P.B., Zhou, H.C., 2011. Carbon dioxide capture-related gas adsorption and separation in metal-organic frameworks. Coord. Chem. Rev. 255 (15–16), 1791–1823.
Li, H.H., Zhang, Q.H., Wang, P., Li, Y.M., Lv, J.X., Chen, W.H., Geng, D.W., Wang, Y.W., Wang, T., Jiang, G.B., 2012. Levels and distribution of hexabromocyclododecane (HBCD) in environmental samples near manufacturing facilities in Laizhou Bay area, East China. J. Environ. Monit. 14 (10), 2591–2597.
Li, Y.J., Miao, J.P., Sun, X.J., Xiao, J., Li, Y.W., Wang, H.H., Xia, Q.B., Li, Z., 2016. Mechanochemical synthesis of Cu-BTC@GO with enhanced water stability and toluene adsorption capacity. Chem. Eng. J. 298, 191–197.
Liang, Z., Marshall, M., Chaffee, A.L., 2009. CO_2 adsorption-based separation by metal organic framework (Cu-BTC) versus zeolite (13X). Energy Fuel 23 (5), 2785–2789.
Lin, S., Song, Z.L., Che, G.B., Ren, A., Li, P., Liu, C.B., Zhang, J.H., 2014a. Adsorption behavior of metal–organic frameworks for methylene blue from aqueous solution. Microporous Mesoporous Mater. 193 (2), 27–34.
Lin, K.Y.A., Yang, H., Petit, C., Hsu, F.K., 2014b. Removing oil droplets from water using a copper-based metal organic frameworks. Chem. Eng. J. 249, 293–301.
Loera-Serna, S., Oliver-Tolentino, M.A., López-Núñez, M.D.L., Santana-Cruz, A., Guzmán-Vargas, A., Cabrera-Sierra, R., Beltrán, H.I., Flores, J., 2012. Electrochemical behavior of $[Cu_3(BTC)_2]$ metal–organic framework: the effect of the method of synthesis. J. Alloys Compd. 540 (11), 113–120.
Marvin, C.H., Tomy, G.T., Armitage, J.M., Arnot, J.A., McCarty, L., Covaci, A., Palace, V., 2011. Hexabromocyclododecane: current understanding of chemistry, environmental fate and toxicology and implications for global management. Environ. Sci. Technol. 45 (20), 8613–8623.
Peng, X.X., Huang, X.Y., Jing, F., Zhang, Z.L., Wei, D.Y., Jia, X.S., 2015. Study of novel pure culture HBCD-1, effectively degrading Hexabromocyclododecane, isolated from an anaerobic reactor. Bioresour. Technol. 185, 218–224.
Petit, C., Bandosz, T.J., 2012. Exploring the coordination chemistry of MOF-graphite oxide composites and their applications as adsorbents. Dalton Trans. 41 (14), 4027–4035.
Saegusa, Y., Fujimoto, H., Woo, G.H., Inoue, K., Takahashi, M., Mitsumori, K., Hirose, M., Nishikawa, A., Shibutani, M., 2009. Developmental toxicity of brominated flame retardants, tetrabromobisphenol a and 1,2,5,6,9,10-hexabromocyclododecane, in rat offspring after maternal exposure from mid-gestation through lactation. Reprod. Toxicol. 28 (4), 456–467.

Schlichte, K., Kratzke, T., Kaskel, S., 2004. Improved synthesis, thermal stability and catalytic properties of the metal-organic framework compound $Cu_3(BTC)_2$. Microporous Mesoporous Mater. 73 (1–2), 81–88.

Solanki, A., Boyer, T.H., 2017. Pharmaceutical removal in synthetic human urine using biochar. Environ. Sci.: Water Res. Technol. 3 (3), 553–565.

UNEP, 2013. Additional Information on Hexabromocyclododecane (HBCD) for Stockholm Covention. Persistent Organic Pollutants Review Committee (POPRC).

Xiao, B., Wheatley, P.S., Zhao, X.B., Fletcher, A.J., Fox, S., Rossi, A.G., Megson, I.L., Bordiga, S., Regli, L., Thomas, K.M., Morris, R.E., 2007. High-capacity hydrogen and nitric oxide adsorption and storage in a metal−organic framework. J. Am. Chem. Soc. 129 (5), 1203–1209.

Xiao, Y.L., Han, T.T., Xiao, G., Ying, Y.P., Huang, H.L., Yang, Q.Y., Liu, D.H., Zhong, C.L., 2014. Highly selective adsorption and separation of aniline/phenol from aqueous solutions by microporous MIL-53(Al): a combined experimental and computational study. Langmuir 30 (41), 12229–12235.

Zhang, Y.H., Tang, Y.L., Li, S.Y., Yu, S.L., 2013. Sorption and removal of tetrabromobisphenol A from solution by graphene oxide. Chem. Eng. J. 222 (8), 94–100.

Zhang, K.L., Huang, J., Wang, H.Z., Liu, K., Yu, G., Deng, S.B., Wang, B., 2014. Mechanochemical degradation of hexabromocyclododecane and approaches for the remediation of its contaminated soil. Chemosphere 116 (15), 40–45.

Zhou, D.N., Wu, Y., Feng, X.N., Chen, Y., Wang, Z.P., Tao, T., Wei, D.B., 2014. Photodegradation of hexabromocyclododecane (HBCD) by Fe(III) complexes/H_2O_2 under simulated sunlight. Environ. Sci. Pollut. Res. 21 (9), 6228–6233.

Zhu, B.J., Yu, X.Y., Jia, Y., Peng, F.M., Sun, B., Zhang, M.Y., Luo, T., Liu, J.H., Huang, X.J., 2012. Iron and 1,3,5-benzenetricarboxylic metal–organic coordination polymers prepared by solvothermal method and their application in efficient As(V) removal from aqueous solutions. J. Phys. Chem. C 116 (116), 8601–8607.

Zukal, A., Opanasenko, M., Rubeš, M., Nachtigall, P., Jagiello, J., 2015. Adsorption of pentane isomers on metal-organic frameworks Cu-BTC and Fe-BTC. Catal. Today 243, 69–75.